Fusion Engineering and Design 192 (2023) 113772

Contents lists available at ScienceDirect

Fusion Engineering and Design

journal homepage: www.elsevier.com/locate/fusengdes

# Structural behaviour characterization of ST40 Inner Vacuum Chamber (IVC2) during a plasma VDE using ANSYS Workbench

S. Carusotti [a,*], R. Lombroni [a], P. Fanelli [a], L. Jackson [c], F. Giorgetti [a,b], P.F. Buxton [c], G. Calabrò [a], M. Romanelli [c], E. Ruiz de Villa Valdes [c]

[a] Department of Economy, Engineering, Society and Business Organization (DEIM), University of Tuscia, Largo dell'Università, Viterbo 01100, Italy
[b] ENEA, Department of Fusion and Nuclear Safety Technology,00044 Frascati, Rome, Italy
[c] Tokamak Energy Ltd, Milton Park, Oxfordshire, UK

ARTICLE INFO

*Keywords:*
Structural analysis
Detailed 3D Model
ANSYS Workbench
ANSYS APDL
ANSA Pre-processor
VDE
Plasma disruption
Tokamak Energy
ST40

ABSTRACT

The paper aims to define the structural behavior of the ST40 Inner Vacuum Chamber (IVC2) under the action of electromagnetic loads from a previously analysed plasma disruption scenario, namely an Upward Vertical Displacement Event (UVDE) scenario. This spherical tokamak is owned by Tokamak Energy Ltd, and it is the highest field device of its kind. The considered loads are obtained from a previous electromagnetic analysis [1] and interpolated on the structural model. Indeed, the study represents the second and final part of the IVC2 electromagnetic and structural behavior characterization. The maximum load due to eddy current and the maximum load generated by halo current (occurring in two different time steps) are studied in two separated analyses. These were carried out considering the entire ST40 model with high degree of detail, allowing to accurately approximate its real behavior and to extrapolate the stress and deformation conditions on all the device elements. Specifically, the completeness of the model has guaranteed to study the global and the local stress state generated on the IVC2, on its supports and on all the components that weigh on it.

## 1. Introduction

Tokamak Energy Ltd. is a privately funded company based in the UK that is presently operating ST40 [2–4]. ST40 is a new generation high field spherical tokamak (ST) whose main design parameters are: $R_0 =$ 0.4 - 0.6 m, $A$= 1.7 - 2.0, $I_{PLA} = 2$ MA, $B_T = 3$ T, $\kappa = 2.5$. ST40 is the highest field device of its kind (until recently STs have typically operated at toroidal field around 0.3 – 0.5 T). An overview of ST40's latest experimental results is provided in [5]. Soon, an important ST40 upgrade is planned and foresees the manufacturing and the installation of a new inner vacuum chamber, called IVC2, that is currently in the final design stage.

In this context, the necessity to characterize in detail the electromagnetic (EM) and structural behavior of IVC2 under the action of critical EM transients, such as plasma disruptions, has recently emerged in order to verify IVC2 design showed in Fig. 1b.

Plasma disruptions [6], often occurring during operations as consequence of transient plasma perturbations [7], are complex phenomena characterized by the abrupt termination of the plasma and the complete transfer of the plasma thermal and magnetic energy to the surrounding structures on very short timescales, with the potential to cause damages in components [6,8]. The evaluation of the disruption-related effects represents one of the main drivers of the design of tokamak components, to ensure they reach the projected lifetime and fulfill their function even in the worst scenario.

This paper deals with the structural assessment of IVC2 under the loads coming from plasma disruptions. In particular, a so-called Upward Vertical Displacement Event (UVDE) fast disruption is here considered. This disruption scenario, fully described in [1], was previously simulated by means of a recently developed methodology based on the use of MAXFEA code in combination with ANSYS. This coupled tool includes an equivalent plasma representation that allows to simulate the plasma evolution during a predefined scenario inside ANSYS. The input data for the 3D EM analysis derives from a previous analysis carried out with MAXFEA code. The main output of this procedure is the evaluation of the EM force density distribution on the different components. This tool was already validated in two different applications for DEMO [9] and for DTT project [10].

* Corresponding author.
*E-mail address:* simone.carusotti@unitus.it (S. Carusotti).

https://doi.org/10.1016/j.fusengdes.2023.113772
Received 31 October 2022; Received in revised form 1 April 2023; Accepted 20 April 2023
Available online 3 May 2023

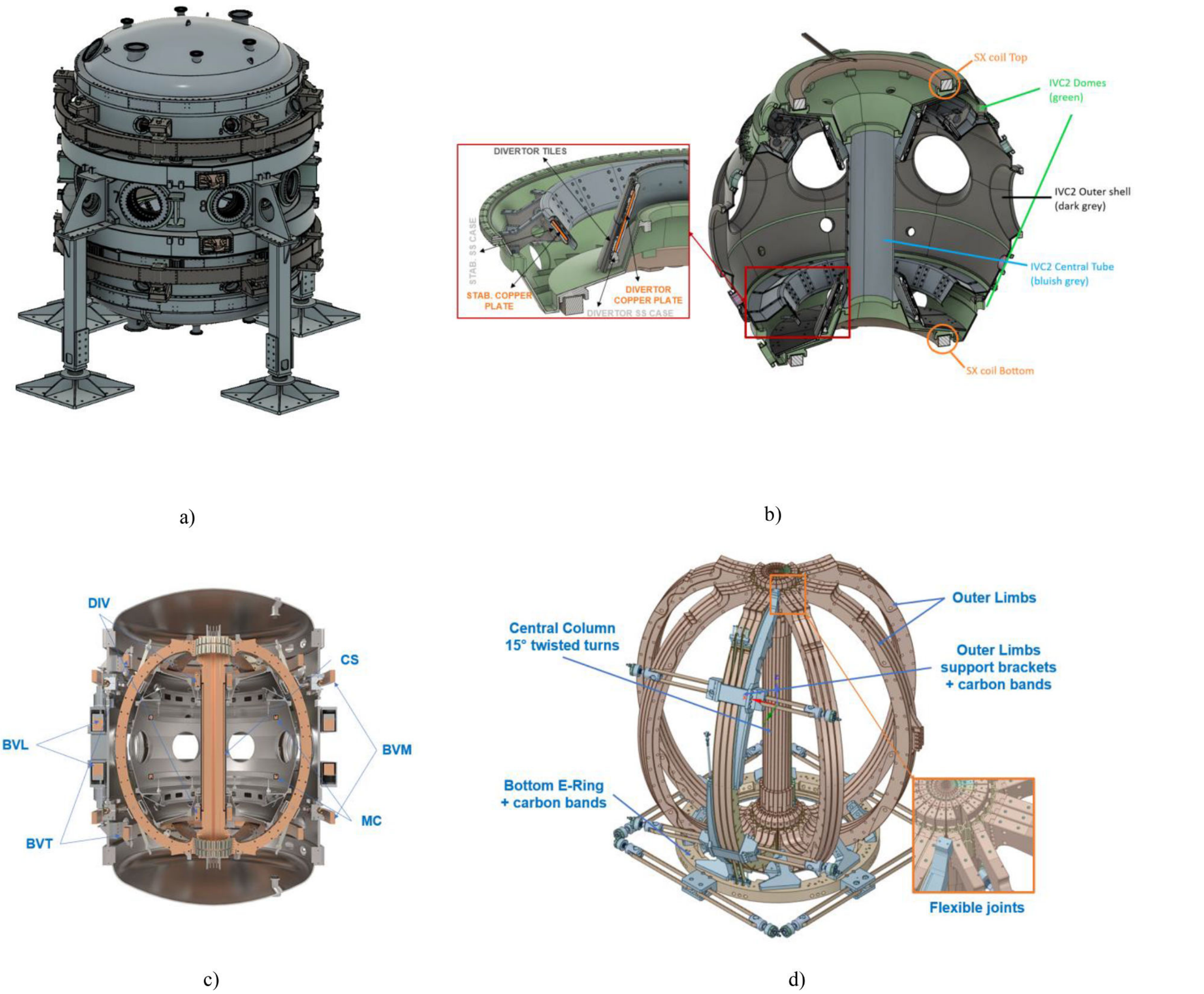


**Fig. 1.** a) ST40 complete CAD model, b) IVC2 overview, c) PF coils system overview and d) TF coils system overview.

Starting from the results of the EM analysis presented in [1], a subsequent structural analysis has been carried out and herein presented. Two characteristic time instants are considered for the structural verification, namely the halo current peak and the eddy current peak time instants. The force density distribution in correspondence of these two instants was firstly extrapolated from the EM model [1], and then used as input for the structural analysis. The latter requires a different mesh specification, level of detail and components. The mesh model is realized using ANSA pre-processor. The model includes more than 100 components and more than 300 joints element, defined through ANSYS APDL code, to reproduce the whole device. The fully mapped mesh model is explained in detail in Section 2. To perform the structural analyses ANSYS Workbench was used. The advantage of using ANSYS Workbench in combination with ANSYS APDL code and ANSA Pre-processor was the possibility to automatically define contacts present in the model and to parametrize the joint elements to the variation of the mesh.

While the main output of this study is the evaluation of the stress state on the IVC2 and on the components that weigh on it, this paper shows the possibility to perform a detailed structural analysis by accurately modeling not only the components of interest. In order to apply this procedure, it is necessary to reduce the model degree of detail by moving away from the focus elements of the analysis reducing the computational resources required. At the same time, it is possible to maintain enough detail to consider the real stiffnesses of all the modelled components and their influence on IVC2. This approach leads not only to the definition of a more accurate and complete stress state on the analysed components, but also allows a solid starting point for future detailed analyses of individual components such as for the TF coils subsystem.

Tokamak structural analyses of this complexity are not common in the literature. The most common approach is to propose single analyses of the individual components. In [10] analyses are carried out considering a high level of detail on the vacuum vessel but including in the structural model the others relevant components only through concentrated forces and moments such as for the divertor; or considering a high detailed model for the divertor and a simplified model for the vacuum vessel and the other elements [11]. Even in [12], authors study the DEMO vacuum vessel dynamic behaviours introducing the in-vessel components as concentrated loads. An additional type of approach provides to use the same mesh for the electromagnetic and structural analysis [13], where the model includes the VV and the plasma facing components (PFCs) and it is used for both analyses. This approach is not always applicable and could lead to non-detailed structural results. In fact, the two analyses require different mesh properties and limits and different geometry simplification to consider [14]. In the context of STs, [15] shows an approach similar to the analysis proposed in this paper, but the mechanical model appears less detailed and containing only the VV.

Instead, this paper is intended to show the feasibility of a structural

a) b)

**Fig. 2.** a) Overview of ST40 global model mesh and its b) poloidal section.

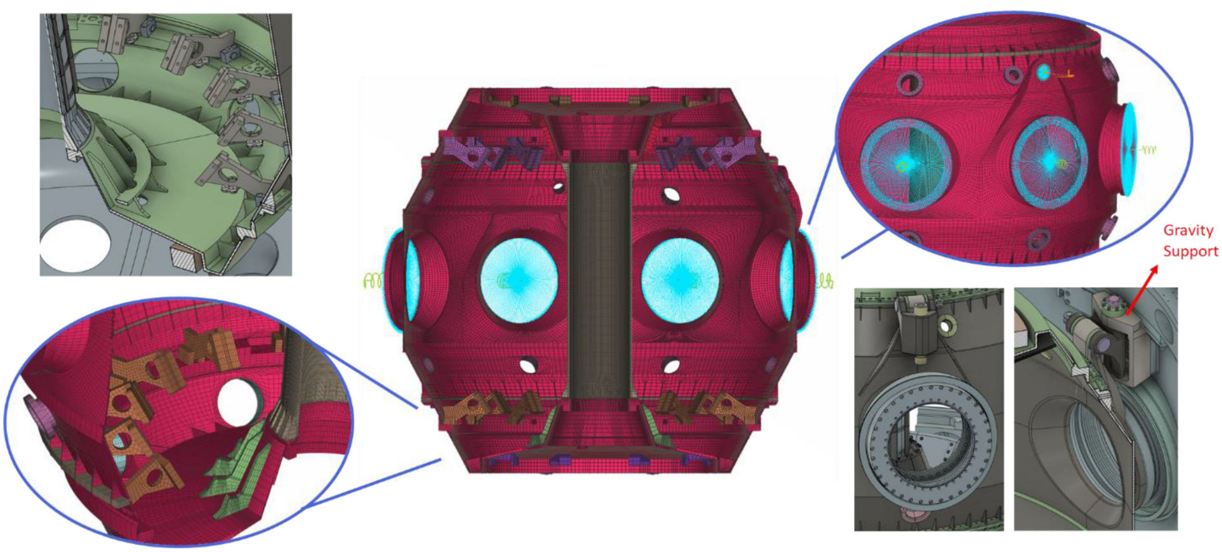


**Fig. 3.** IVC2 mesh model with a zoom on the stabilization plate and divertor zone and a detail of the equivalent elements for the bellows (COMBIN7 in light green) and for the gravity supports (MPC184 General element in orange).

analysis considering a complete model of a tokamak. The advantage of this modeling methodology is the possibility to verify the IVC2 including the stiffness of all the components affecting its stress state. With this approach, it is possible to achieve an accurate precision in the assessment of the stress state. At the same time, it leads to an overview of the stress state on the whole ST40 IVC2 model enabling to highlight other possible critical zones. In addition, with the proposed model it is possible to obtain the input data, such as the stress state or the displacement, needed for more detailed analyses focused on single components.

## 2. ST40 detailed model

ST40 consists of four main sub-assembly: the IVC2 system, the OVC system and the toroidal and poloidal field (TF and PF) coils system [6]. The OVC is a structure that mechanically supports the IVC2, PF and TF coils components. It is supported by four legs and the entire assembly sits on top of the assembly platform (not reported in Fig. 1a). The IVC2 is connected to the OVC through eight bellows and four gravity supports, these latter prevent all displacements and keep free the rotations. A couple of up-down symmetric divertors and stabilizing plates, encapsulated in a jacket, are connected to IVC2 through their supports properly modelled. The graphite and molybdenum limiter tiles that covered the IVC2 and the divertor and stabilizing case are not considered in the model. Regarding the ST40 TF and PF coils, they are all made of copper. Concerning the PF coils, ST40 presents five pairs of coils, namely the BVL, BVM, BVU, SX and DIV coils, for the plasma current, position and shape control (showed in Fig. 1c). ST40 has also a Central Solenoid (CS) directly wounded on the TF central column. For the plasma startup ST40 uses a process called Merging Compression (MC) [16,17],. For that purpose, two in-vessel MC coils are installed together with a pair of push (PSH) coils located outside the IVC2. The SX, DIV, MC and PSH coils are connected to the IVC2 through their casing, while the BVL, BVM and BVU coils are fixed to the OVC.

The TF coils system, showed in Fig. 1d is composed by central column and 24 outer limbs connected with flexible conductive joints. The

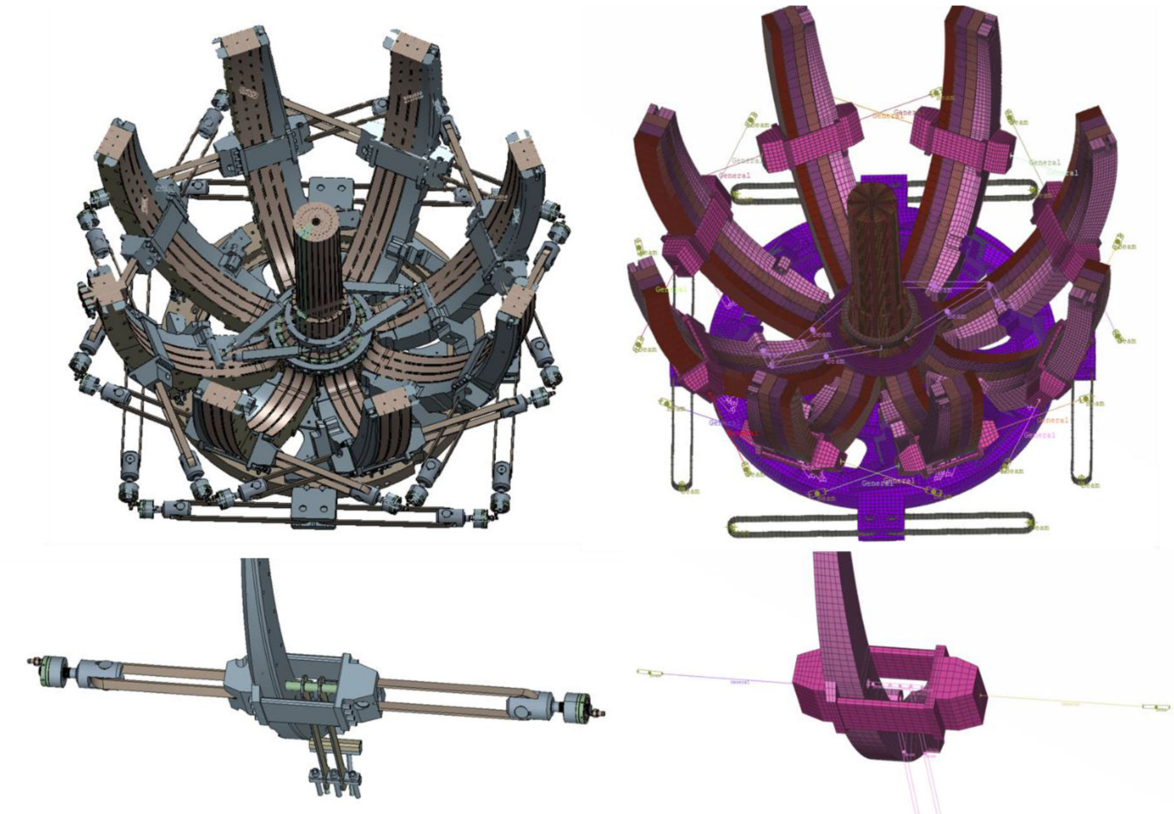

a)

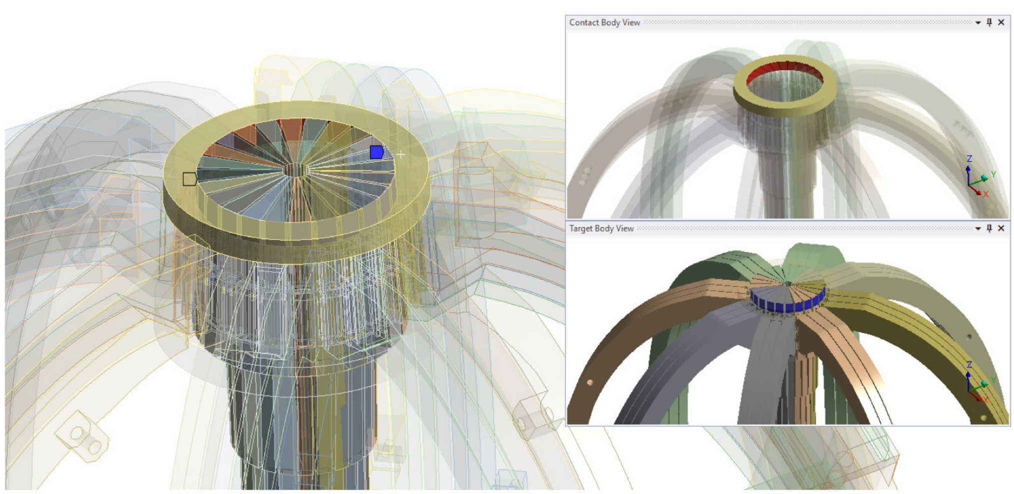


b)

**Fig. 4.** a) Comparison between the TF coils restraint systems and its equivalent model through MPC184 General and Beam element b) Compressional ring contacts definition with an equivalent interference.

central column is also composed of 24 wedges with a 15° twisted in the central part to allow connecting one TF turn to the next, while in the outer zone the turns are arranged in 8 limbs with 3 turns in each. This system presents connections with the OVC on the outer limbs with two support brackets (top and bottom), connected to the OVC with two carbon fiber straps each. In addition, there are two plates, one at the top and one at the bottom of the device (namely the E-Ring), with eight carbon fiber straps each, to add extra support against twisting. The TF coils system also present two torsional rings that prevent the torque between the central column and the outer limbs, and two compressional rings holding in position the central column elements.

The structural model has been developed considering the whole 360° of ST40, in fact one of the 4 OVC legs is tilted approximately 7° from its symmetrical position; this does not allow the realization of a symmetrical model to reduce the computational resources required. The mapped mesh consists of 4310k nodes and 3341k of SOLID185 bricks and wedge elements. This high-quality model allows to work with a non-excessive nodes number reducing the required computational

**Table 1**
Overall forces resulting on the entire model following the EM load interpolation.

| | Eddy current peak time instant | Halo current peak time instant |
|---|---|---|
| $F_x$ [N] | $-3.501 \times 10^2$ | $-2.980 \times 10^2$ |
| $F_y$ [N] | $9.618 \times 10^1$ | $1.071 \times 10^2$ |
| $F_z$ [N] | $3.990 \times 10^5$ | $3.315 \times 10^5$ |

resources (~2 h required for each analysis, post-processing including, run on UNITUS server RAM 128 GB, 12 processors, i9–10,920 @ 3.50Ghz). The model holds more than 100 components connected through 450 bonded contacts automatically set in ANSYS Workbench and with more than 300 joints elements defined with APDL code. An overview of the whole mesh in provided in Fig. 2a and b.

### 2.1. IVC2 system

This system represents the main part of interest of the analysis, in fact its components achieve the highest degree of detail of the whole model. Indeed, the mesh model includes 1426k nodes and 1097k elements namely the 33% of the whole ST40 mesh model. The high detailed mesh of the IVC2 is showed in Fig. 3.

The IVC2 connection components with the OVC have been simplified into ANSYS APDL elements, allowing to greatly simplify the connection zones on the OVC maintaining the information on the load transfer between each other. Indeed, the bellows are simulated with COMBIN7 elements which present an equivalent stiffness; while the IVC2 gravity supports are modelled through a MPC184 General element with all the displacements fixed, while all rotations are kept free. These elements are connected to the IVC2 through the CERIG command that generate a rigid connection between the selected nodes. The IVC2 connections with the

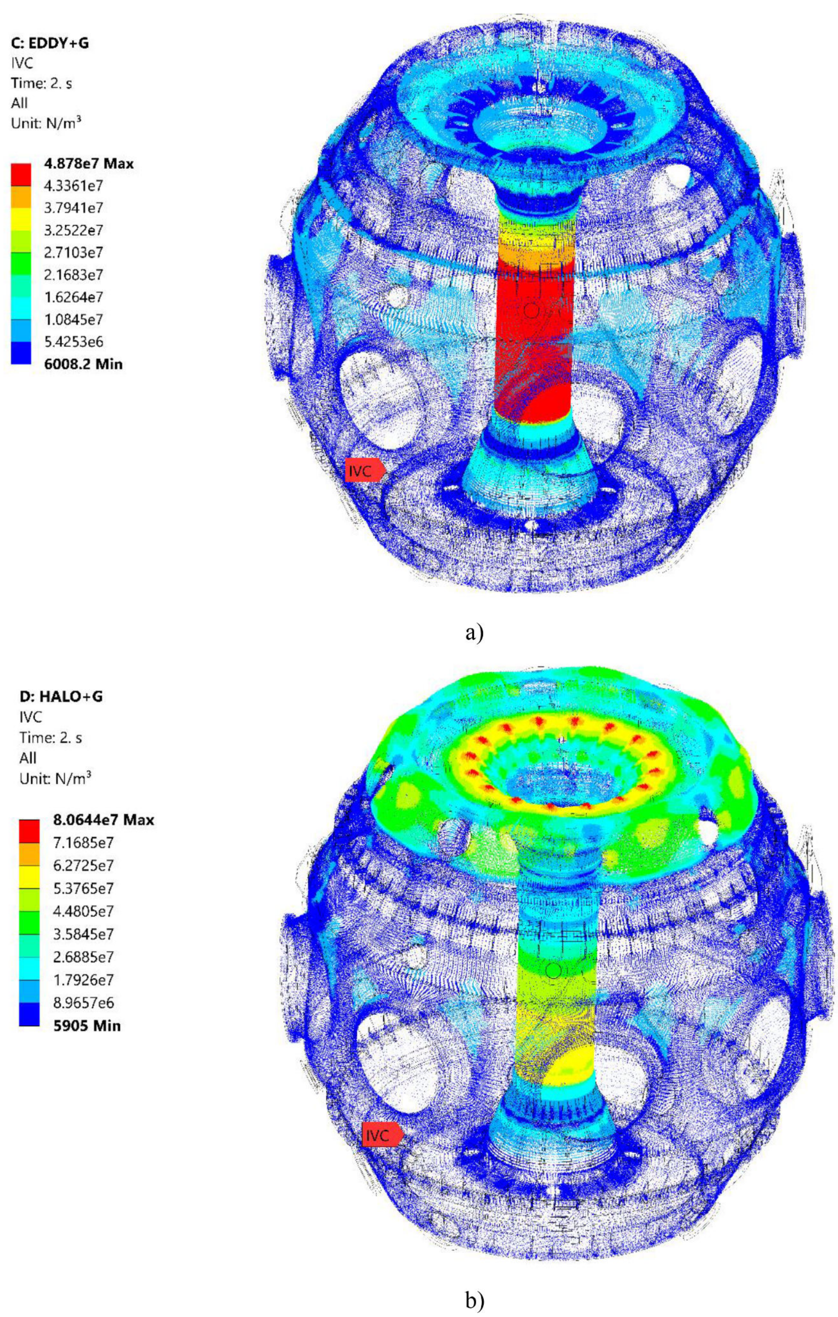


**Fig. 5.** Body force density related to the a) eddy current and b) halo current peak time instant.

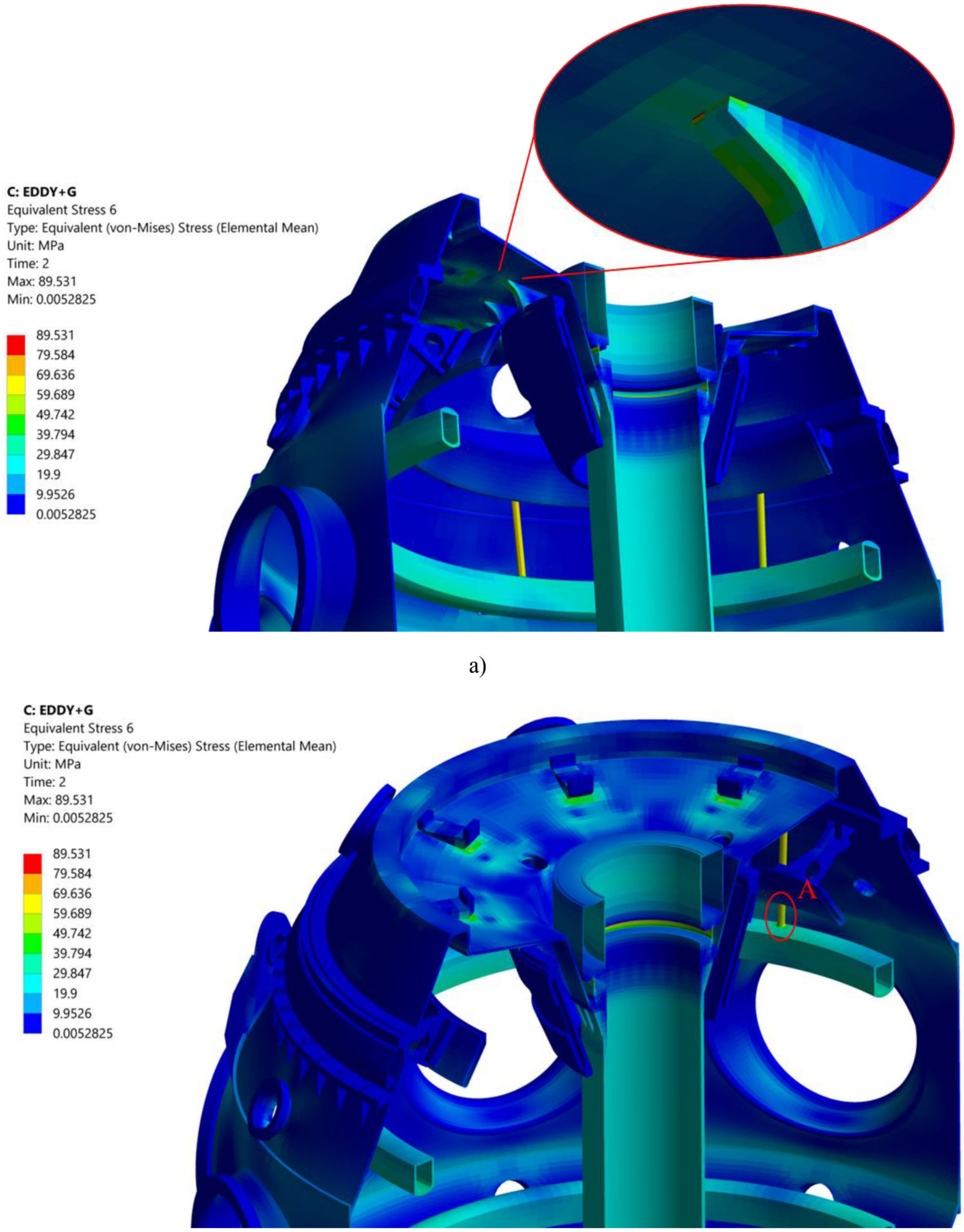


b)

**Fig. 6.** Von Mises stress contour at the eddy current peak on the IVC2 and the In-Vessel components. Focus on a) the stress peak and b) the other most stressed components; c) overview on the stress state.

OVC are showed in Fig. 3.

The divertor supports and the SX coils supports are connected to the IVC2 structure through the mesh nodes, while the stabilizing plate supports, the MC, PSH and DIV casing are connected to it with a bonded contact. Also, the IVC2 flanges are connected through the mesh nodes; this type of connection reduces the computation resources required compared with a bonded contact (MPC equation).

### 2.2. OVC system

The OVC sustains all the other ST40 sub-assembly and discharges to the ground all the acting load (including the gravity force) on the reactor through its four legs. The legs are not arranged symmetrically with respect to the device central axis, indeed one of these results twisted by $\sim 7^{\circ}$ causing a different stress state between them.

The final plate is constrained to the ground with a ANSYS Workbench fixed support. To simplify the connections between the OVC legs and its final plate a MPC184 Beam element was introduced; in the real model there are also elements useful for vibration damping, but since the aim of this paper is to carry out a static structural analysis these are neglected. Also, in this case the connection between the beam element and the OVC leg is carried out thanks to the CERIG command.

To ensure greater resistance in the areas of connection with the TF coils system, the structure of the OVC provides four massive rings on which connect the carbon fiber straps.

 

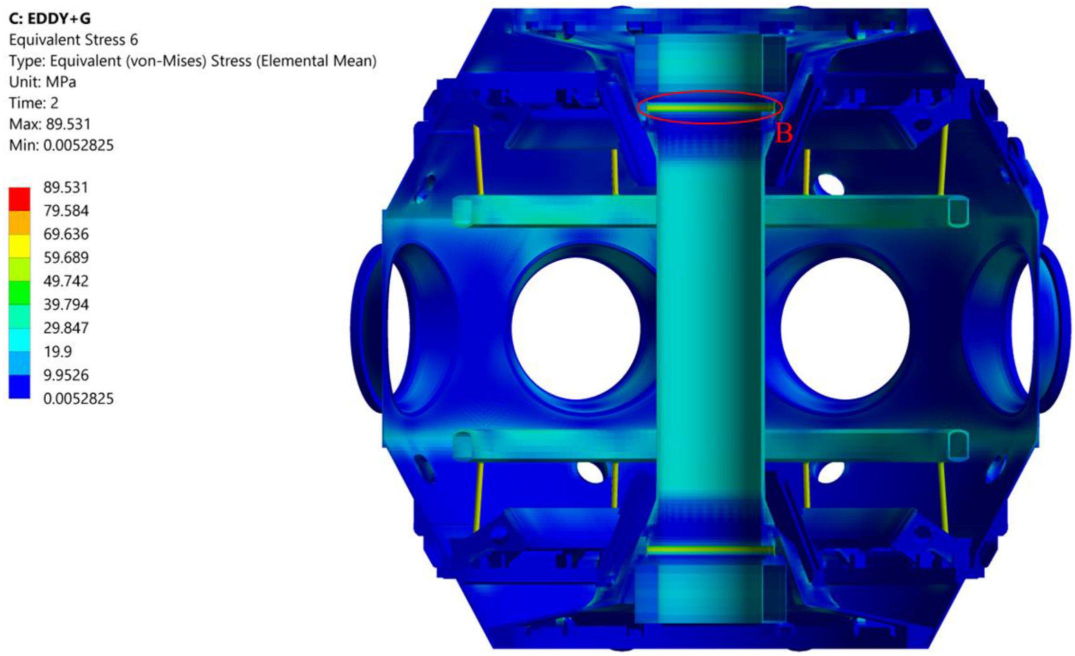


c)

**Fig. 6.** (*continued*).

### 2.3. PF coils system

The PF coils system includes all the magnets, their insulating and the supports or casing not connected to the IVC2. The coils connections with IVC2 and OVC are realized with bonded contact and fixed joints set in Ansys Workbench. The CS is set fixed to the TF central column to reproduce the real connection.

For greater compatibility with electromagnetic loads [1] the passive coils (MC and PSH coils) are modelled as set of filaments, while the active coils are modelled as a larger single filament. Consequently, the insulating components are modelled to fill the space between the coils and their casing. To simplify the connection between BVL coils and their casing, a MPC184 Beam element constrained with a CERIG command is used. Moreover, the BVL casings are connected to the OVC with a MPC184 Beam elements. In addition, between the BVL casings and the OVC legs are set a bonded contact.

### 2.4. TF coils system

This system represents the most complex ST40 sub-assembly in term of number of number of joints, connections, and constraint element.

To connect the outer limb with the central column ST40 use an elastic joint composed of multiple copper sheets packed together. In fact, the real aim of these components is the electrical connection without any structural role. To simplify the analyses, this joint is considered as composed of solid copper introducing an additional stiffness that will cause an overestimated stress state.

The carbon fiber straps for the connection of TF outer limb with OVC are simulated with MPC184 General elements with an equivalent stiffness. The additional carbon fiber straps connected to the E-Ring are modelled respecting the real geometry. The different modeling of this element allows to simplify the mesh on the TF coils supports. The connections between each carbon fiber straps and the OVC are modelled through MPC184 Beam element, also in this case the simplification of this connection allow to realize more easily the OVC mesh model without lost any information on the transfer loads. The comparison between the TF coils restraint systems and its equivalent model is showed in Fig. 4a. A 168 kN pretension forces is applied on all fiber straps with a couple of nodal forces.

All push and pull rods, used to increase the TF coils stiffness, are simulated through MPC184 Beam element connected to the outer limbs and to the E-Ring with a rigid zone (CERIG command). The outer limbs are interconnected with a fixed joint that simulate the real bolt connection. The torsional constraints system connected to the central column is simulated through a rigid ring linked to the outer limbs support using a MPC184 Beam element. The compressional preloaded rings are simulated with a rigid ring connected to the TF magnets central column. An equivalent interference contact is introduced to reproduce the real preload, namely 40 kN and 75 kN on outer and inner rings respectively (Fig. 4b).

## 3. Analysis pre-setting

### 3.1. Materials

The materials used for the analysis are:

- AISI-316L - used for the IVC2 central tube, for all the PF coils casing and supports, for the OVC including the legs and for the TF coils supports;
- Inconel 718 – used for the IVC2 domes and outer shell;
- Copper Alloy – used for the PF and TF coils;
- Titanium Alloy – used for the E-Ring;
- G10 – used for the insulating components;
- Carbon PEEK – used for the carbon fiber straps.

The analyses are carried out considering an average environment temperature of 20 °C, the different operating temperatures are considered into the allowable stress for the materials. The material proprieties of the AISI-316 L and for the Inconel 718 were extracted from ITER SDC-IC code for Structural Analysis of the ITER In-vessel components (Appendix A) [18].

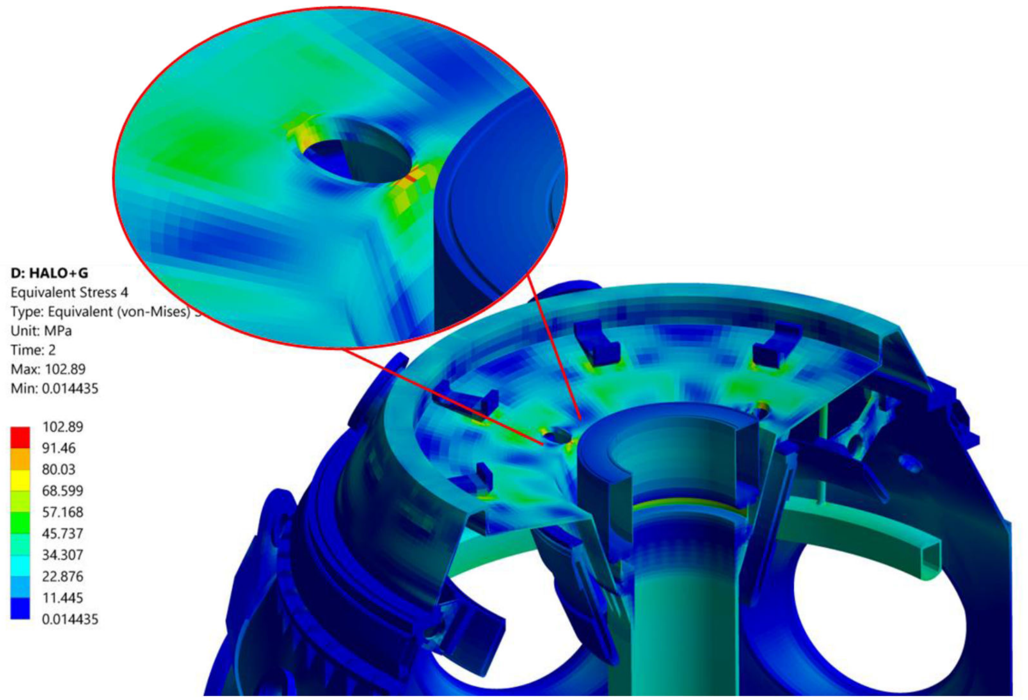


a)

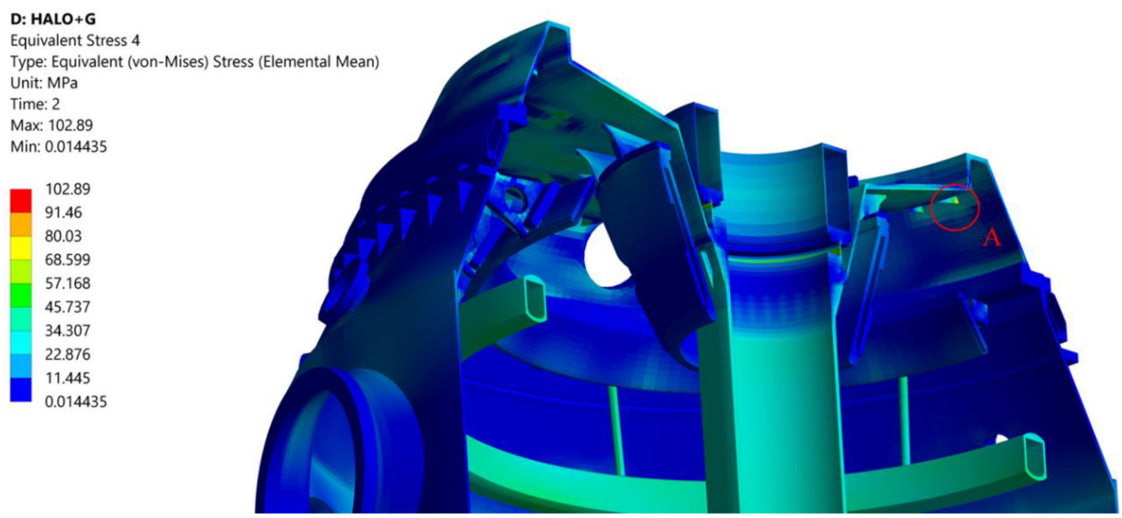


b)

**Fig. 7.** Von Mises stress contour at the halo current peak on the IVC2 and the In-Vessel components. Focus on a) the stress peak and b) the other most stressed components; c) overview on the stress state.

### *3.2. Loads interpolation*

The EM loads acting on the structure are interpolated from the EM models and applied as body force densities on the Structural Model by means of the distance based average method. This is a simple robust method that uses the distance from the target node to the specified number of closest nodes to calculate a weighting value [19]. The interpolated values on structural model (target mesh) are calculated using only three nodes within a spherical region of influence with a radius of 20 mm. Such methodology allows to reach the 99% (554,470 of 556,232) of nodes mapped on the IVC2 target mesh in less than 1 s.

The overall forces acting on the entire model were used as a metric to verify the goodness of the interpolation performed. In Table 1 are reported the overall forces obtained from the interpolation method proposed. These forces comply with the condition of maximum error of 10% between the input EM loads and the force density distribution obtained on the structural model. The force density distribution for the IVC2 is showed in Fig. 5. The force density distribution obtained from the interpolation is used as input for the structural analyses of each component.

## 4. Results

### *4.1. Eddy current peak instant (0.0674s)*

This time instant corresponds to the maximum value of the eddy

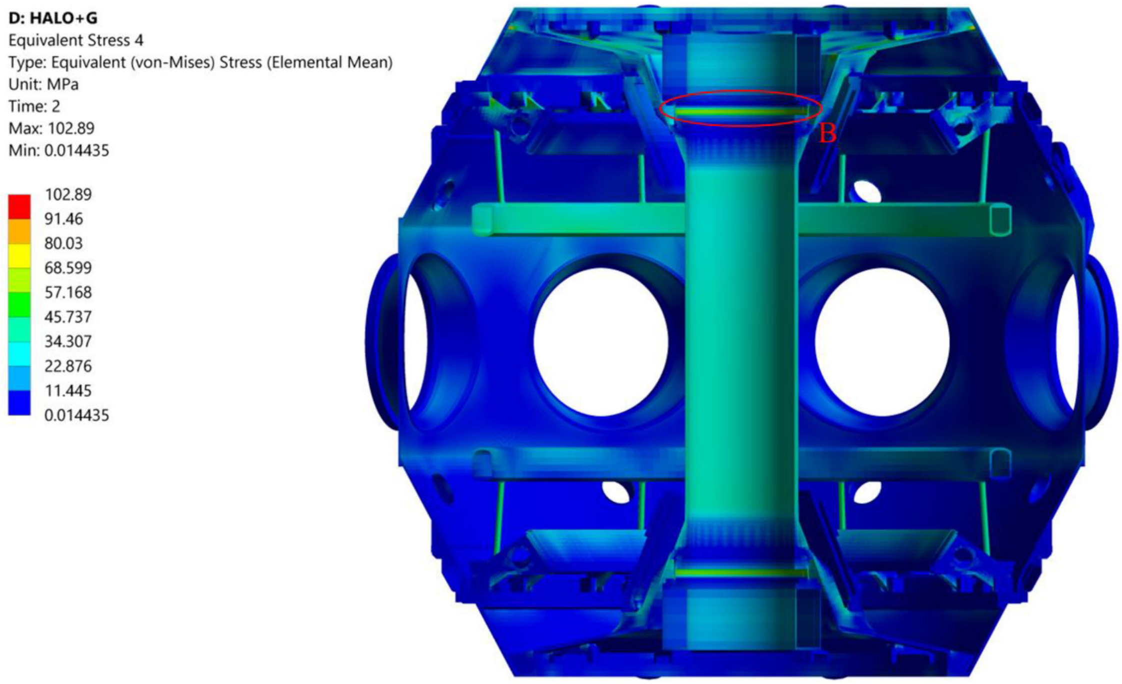


c)

**Fig. 7.** (*continued*).

current induced in the structures, occurring at the end of CQ. The simulation also considers the gravity load. An overview of the von Mises stress contour on the IVC2 and the In-Vessel components is given in Fig. 6c. It is possible to observe how the von Mises stress is well below allowable primary membrane stress intensity of materials considering a constant temperature of 80 °C (126.7 MPa for the SS 316 L and 690 MPa for the Inconel 718) obtained considering the ITER SDC-IC code for Structural Analysis of the ITER In-vessel components (Level A criteria) [18]. The stress peak value is obtained in the top Divertor support (89.5 MPa) as showed in Fig. 6a. This stress concentration is due to the pull forces acting on the divertor and its casing. The other most stressed components are the MC coils support (~65 MPa highlighted in Fig. 6b-A) and the DIV coils connection with the IVC2 (~55 MPa highlighted in Fig. 6c-B) as showed in Fig. 7b.

### 4.2. *Halo current peak instant (0.0668s)*

This time instant corresponds to the maximum value of the halo current induced in the structures. The simulation also considers the gravity load. An overview of the von Mises stress contour on the IVC2 and the In-Vessel components is given in Fig. 7c. It is possible to observe how the von Mises stress is well below allowable primary membrane stress intensity of materials considering a constant temperature of 80 °C (126.7 MPa for the SS 316 L and 690 MPa for the Inconel 718) obtained considering the ITER SDC-IC code for Structural Analysis of the ITER In-vessel components (Level A criteria) [18]. The stress peak value (102.9 MPa) is obtained of the holes in the top Dome caused by a stress concentration as showed in Fig. 7a. The other most stressed components are the Dome ribs (~80 MPa - A), where is generated another stress concentration, and the DIV coils connection with the IVC2 (~70 MPa - B) as showed in Fig. 8b. As expected, the Stabilization plate and Divertor supports are more stressed with respect to the Eddy current peak time instant due to the Halo current flow.

## 5. Conclusions

In this paper the fully 3D structural analysis of ST40 is carried out to verify the structural behavior of its new vacuum chamber IVC2 during an UVDE fast disruption. For this purpose, a high detailed mesh model is realized. The model includes all main components of ST40 and it considers their real stiffnesses influence on IVC2 and the components that weigh on it. The EM load derives from a previous analysis carried out with the combination of MAXFEA code and ANSYS APDL and integrally described in [1].

From the EM analysis two critical time instants have been identified and studied, namely the eddy peak and the halo peak instants. The von Mises stress in the IVC2 and in the In-Vessel Components is found below the allowable primary membrane stress intensity in both the simulations. The most critical zones are highlighted in the Halo peak simulation: a peak of 102.9 MPa due to the stress concentration in the holes located in the top Dome and a peak of ~80 MPa in correspondence of the top Dome ribs. For the Eddy peak simulation, the stress peak of 89.5 MPa is obtained in the top Divertor support.

In conclusion, this study demonstrates the applicability of the proposed procedure to complex models with a high level of detail and high number of elements. In addition, the proposed global analysis is a starting point for future detailed analysis of further components of interest.

## CRediT authorship contribution statement

**S. Carusotti:** Conceptualization, Methodology, Software, Validation, Formal analysis, Investigation, Data curation, Visualization, Writing – original draft, Writing – review & editing. **R. Lombroni:** Software, Validation, Formal analysis, Data curation, Visualization, Writing – review & editing. **P. Fanelli:** Conceptualization, Resources, Supervision, Project administration, Funding acquisition, Writing – review & editing. **L. Jackson:** Conceptualization, Resources, Supervision, Writing – review & editing. **F. Giorgetti:** Conceptualization, Methodology, Software, Validation, Formal analysis, Visualization, Data curation, Writing

– review & editing. **P.F. Buxton:** Conceptualization, Resources, Supervision, Project administration, Funding acquisition, Writing – review & editing. **G. Calabrò:** Conceptualization, Resources, Supervision, Project administration, Funding acquisition, Writing – review & editing. **M. Romanelli:** Conceptualization, Resources, Supervision, Project administration, Funding acquisition, Writing – review & editing. **E. Ruiz de Villa Valdes:** Conceptualization, Resources, Writing – review & editing, Supervision.

## Declaration of Competing Interest

The authors declare that they have no known competing financial interests or personal relationships that could have appeared to influence the work reported in this paper.

## Data availability

The data that has been used is confidential.

## References


[1] R. Lombroni, S. Carusotti, et al., Use of MAXFEA code in combination with ANSYS APDL to study the Electro-Magnetic behaviour of the new ST40 Inner Vacuum Chamber (IVC2) proposal during a plasma VDE, Fusion Eng. Des. 192 (2023).

[2] A. Sykes, et al., Compact fusion energy based on the spherical tokamak, Nucl. Fusion 58 (1) (2018).

[3] M. Gryaznevich, Faster fusion: ST40, engineering, commissioning, first results, AIP Conf. Proc. 2179 (November 2019).

[4] M. Gryaznevich, O. Asunta, Overview and status of construction of ST40, Fusion Eng. Des. 123 (2017) 177–180.

[5] S. McNamara, et al., Overview of recent results from the ST40 high-field spherical Tokamak, Bull. Am. Phys. Soc. 66 (2021).

[6] F.C. Schuller, Disruptions in tokamaks, Plasma Phys. Control. Fusion 37 (11A) (1995).

[7] G. Sias, et al., Inter-machine plasma perturbation studies in EU-DEMO relevant scenarios: lessons learnt for EM forces prediction during VDEs, Nucl. Fusion 62 (7) (2022).

[8] M. Sugihara, et al., Disruption scenarios, their mitigation and operation window in ITER, Nucl. Fusion 47 (4) (2007) 337–352.

[9] R. Lombroni, F. Giorgetti, et al., Using MAXFEA code in combination with ANSYS APDL for the simulation of plasma disruption events on EU DEMO, Fusion Eng. Des. 170 (2021).

[10] F. Giorgetti, R. Lombroni, et al., Vertical displacement events analysis using MAXFEA code in combination with ANSYS APDL in the final design stage of the DTT Vacuum Vessel, Fusion Eng. Des. 184 (2022).

[11] G. Di Mambro, et al., Mechanical impact of electromagnetic transients on the European DEMO divertor. Part 1: vertical displacement event, Fusion Eng. Des. 175 (2022).

[12] F. Giorgetti, et al., Dynamic behaviour of DEMO vacuum vessel during plasma vertical displacement events, Fusion Eng. Des. 159 (2020).

[13] L. Sumei, et al., Electromagnetic and structure analysis for EAST vacuum vessel with plasma facing components during VDE, Fusion Eng. Des. 124 (2017).

[14] J. Zhu, et al., Specific features of eddy current analysis with ANSYS® for fast plasma current decay event in W7-X, Fusion Eng. Des. 163 (2021).

[15] M. Awais, et al., Effects of structural and electromagnetic loads on vacuum vessel of Pakistan spherical Tokamak, Fusion Eng. Des. 168 (2021).

[16] M. Gryaznevich, A. Sykes, Merging-compression formation of high temperature tokamak plasma, Nucl. Fusion 57 (7) (2017).

[17] P.F. Buxton, et al., Merging compression start-up predictions for ST40, Fusion Eng. Des. 123 (2017).

[18] ITER SDC-IC, Materials design limit data, Iter_222RLN. (Private Communication).

[19] D. Shepard, "A two-dimensional interpolation function for irregularly-spaced data", *Proceedings of the 1968 ACM National Conference.*